Conditions for the appearance of wave chaos in quantum singular systems with a pointlike scatterer

T. Shigehara
Computer Centre, University of Tokyo, Yayoi, Bunkyo-ku, Tokyo 113, Japan
(Received 20 June 1994)

In this paper, we discuss quantum properties of singular systems with a single pointlike scatterer that are almost integrable (pseudointegrable). Special emphasis is placed on the investigation of the appearance of so-called wave chaos. Based on a general argument, we deduce the necessary condition for the appearance of wave chaos in singular systems with a pointlike scatterer. Numerical results of a rectangular billiard with a single pointlike scatterer show that the signature of wave chaos is observed in various energy regions according to the value of the coupling constant of the scatterer, as expected from the general argument.

PACS number(s): 05.45.+b

I. INTRODUCTION

Chaos can be rigorously defined in classical mechanics. The essential mechanism which brings about chaos is known to be the stretching and folding mechanism [1–4]. Stretching occurs along unstable directions, while folding occurs along stable directions. The average magnitude of the stretching is expressed by the Lyapunov exponent. We can regard deterministic systems as chaotic if and only if the Lyapunov exponent is positive.

Contrary to classical mechanics, persistent stretching and folding does not seem to occur in quantum mechanics. From the viewpoint of algorithmic complexity [5], it is known that autonomous bounded quantum systems are not chaotic in general. Even in a kicked rotator, which is a driven system, it is observed [6] that the quantum energy never persistently diffuses as it does classically. The main concerns of studying chaos in quantum mechanics, which is often abbreviated as *quantum chaos,* do not consist in seeking persistent stretching, but in understanding generic quantum properties of quantized classically chaotic systems. It is considered one of the main aspects of *quantum chaology* [7,8] to understand, in terms of quantum mechanics, the necessary and sufficient conditions for deterministic systems to be classically chaotic.

Concerning autonomous bounded systems, a large number of theoretical and numerical studies have been performed and have revealed an intimate relation between the quantum spectrum (energy levels and wave functions) and the underlying classical dynamics. There is a conjecture that the local level statistics for classically chaotic systems are well described in terms of random matrix theory [9,10]. In particular, if the Hamiltonian has a time reversal symmetry, the level statistics are described in terms of a Gaussian orthogonal ensemble (GOE). This is in sharp contrast with the level statistics for classically integrable systems, which are described by Poisson statistics in generic case [11].

Quantum aspects of so-called *almost integrable* [12] (*pseudointegrable* [13]) billiards have attracted renewed attention in recent years [14]. Rational polygons or rectangular staircases are typical examples of such billiards. From the classical viewpoint, almost integrable systems can be considered as integrable in the sense that all orbits are stable except unstable orbits which are of measure zero. A straightforward application of the correspondence between the level statistics and the classical dynamics implies that the level statistics of almost integrable systems are not substantially different from Poisson statistics. Some numerical studies have, however, revealed that this is not the case. It is observed in rectangular staircases [15] that the level statistics gradually approach GOE predictions as the number of steps increases. The level statistics close to GOE predictions are also observed in rational polygons [16]. Indeed, it has been recently asserted [17] that finite mathematics is indispensable for understanding the physics of rational polygons and indicates that such polygons can actually have a positive Lyapunov exponent, contrary to assertions based on continuum mathematics.

Another interesting example of almost integrable systems is a singular billiard with a single pointlike scatterer, which is obtained by attaching a pointlike obstacle to an integrable billiard. One of the specific features of such singular systems is that they have an additional system parameter, that is, the coupling constant of the scatterer, which does not exist for rational polygons or rectangular staircases. (We will later introduce two kinds of coupling constants in this paper: the *bare coupling constant* and the *physical coupling constant.* Unless there is danger of confusion, the former is merely referred to as the coupling constant.) The authors of Ref. [18] have examined the case of a rectangular billiard and observed that the chaotic spectrum emerges if the coupling constant of the scatterer is large enough. This phenomenon has been called *wave chaos* because its appearance is attributed to purely quantum effects: owing to the uncertainty principle, the pointlike particle moving in the billiard gains a "size" and indeed hits the pointlike obstacle. Despite the plausible and attractive notion of wave chaos, the authors of Ref. [19] have recently noticed that the basis taken into account in the calculation in Ref. [18] is overly truncated and have shown that the level statistics never approach GOE predictions even if the coupling constant is

infinite.

One of the main purposes of this paper is to give a definite answer to questions concerning rectangular billiards with a single pointlike scatterer, particularly whether or not wave chaos exists and, if it exists, what the condition is for its appearance. To this end, we consider a general case where a single pointlike scatterer is attached to an autonomous bounded integrable system, and deduce the necessary condition for the appearance of wave chaos. In Sec. II we briefly review a rigorous treatment for singular systems with a pointlike scatterer which is based on self-adjoint extension theory. A coupling constant of the scatterer, which will be referred to as the *bare coupling constant* in this paper, will be formally defined in a natural way following this theory. Some general properties of singular systems with a pointlike scatterer are clarified in Sec. III. First, we examine a simple one-dimensional case in order to extract the physical meaning of the bare coupling constant. We will see that it is not a direct measure of the strength of the scatterer in the physical sense. We then attempt to define another coupling constant of the scatterer in such a way that it directly represents the physical strength of the scatterer. It will be referred to as the *physical coupling constant* in this paper. It will be shown that things are quite different according to whether $\alpha<0$ or $0\leq\alpha<1$, where α is defined so that the average level density of the integrable system is $\rho_{\rm av}(E)\sim E^{\alpha}$ for large energy E. While the physical coupling constant can be defined in a straightforward manner for $\alpha<0$, this is not the case for $0\leq\alpha<1$. Introducing an *effective basis;* however, we obtain the condition for the physically strong coupling for the latter case. A remarkable feature in the case of $0\leq\alpha<1$ is that the energy region where the physically strong coupling emerges is different according to the value of the bare coupling constant. We apply, in Sec. IV, the general consideration made in the preceding section to a rectangular billiard with a pointlike scatterer. The validity of our argument is confirmed numerically. The quantum spectrum of this system is also investigated in detail. It will be shown that wave chaos indeed appears under the appropriate condition expected from the general argument. Furthermore, the results obtained in some previous papers are reexamined from the present point of view. We summarize the present work in Sec. V.

II. FORMALISM

Several methods are known for solving problems with a singular (zero-range) scatterer in quantum mechanics [20,21]. One of them is based on *self-adjoint extension theory,* originally developed by von Neumann. Its applications for bounded singular systems are given in Refs. [18,22]. In this section, we will give a brief sketch of the formalism, restricting ourselves to necessary points for the following discussion. It can readily be seen that a coupling constant of the singular scatterer is formally introduced in a natural way following the theory.

Suppose that an autonomous bounded integrable system with the Hamiltonian H_0 is given. Let E_n and $\varphi_n(\mathbf{x})$ $(n=1,2,3,\ldots)$ be the energy eigenvalues and the corresponding eigenfunctions of H_0, respectively,

$$H_0\varphi_n(\mathbf{x})=E_n\varphi_n(\mathbf{x}) \ . \tag{1}$$

The domain of H_0, $D(H_0)$, is a set of square-integrable functions with an appropriate boundary condition. The Green's function of the integrable system is given by

$$G^{(0)}(\mathbf{x},\mathbf{y};z)=\sum_{n=1}^{\infty}\frac{\varphi_n(\mathbf{x})\varphi_n(\mathbf{y})}{z-E_n} \ , \tag{2}$$

where z is the energy variable.

We now proceed to attach a pointlike obstacle to the integrable system. The first step for this is to remove the relevant scattering point $\mathbf{x}_0$. This is done by restricting H_0 to $H_0\lceil D$ with the domain

$$D=\{\varphi(\mathbf{x})\in D(H_0)\,|\,\varphi(\mathbf{x}_0)=0\} \ . \tag{3}$$

It is a straightforward matter to prove that $H_0\lceil D$ is a *symmetric (Hermitian)* operator but not a *self-adjoint* operator. In general, a self-adjoint operator is a symmetric operator. The converse is, however, not necessarily valid. The self-adjointness is required for the Hamiltonian in quantum mechanics in order to ensure the unitarity of the time evolution operator. The general prescription for *extending* a symmetric operator to self-adjoint operators is given within the framework of self-adjoint extension theory. The theory tells us that if

$$\sum_{n=1}^{\infty}\frac{1}{E_n^2+1}<+\infty \ , \tag{4}$$

then all of the self-adjoint extensions of $H_0\lceil D$ are given by a one-parameter family of the Hamiltonian

$$H_{\Theta}=H_0 \ , \tag{5}$$

with the domain

$$D(H_{\Theta})=\{\psi(\mathbf{x})\,|\,\psi(\mathbf{x})=\varphi(\mathbf{x})+cG^{(0)}(\mathbf{x},\mathbf{x}_0;+i)-ce^{i\Theta}G^{(0)}(\mathbf{x},\mathbf{x}_0;-i);\varphi(\mathbf{x})\in D,c\in\mathbb{C},0\leq\Theta<2\pi\} \ . \tag{6}$$

The condition of Eq. (4) can be rewritten in terms of the average level density of the unperturbed integrable system, $\rho_{\rm av}(E)$, as follows:

$$\int_0^{\infty}\frac{\rho_{\rm av}(E)}{E^2+1}dE<+\infty \ . \tag{7}$$

This indicates that if

$$\rho_{\rm av}(E)\sim E^{\alpha} \ , \tag{8}$$

for large energy E, then $\alpha < 1$ is required.

Let us suppose in the following that $\alpha < 1$ holds. In this case, it is known that the Green's function for the system with the Hamiltonian H_Θ is given by

$$G_\Theta(\mathbf{x},\mathbf{y};z)=G^{(0)}(\mathbf{x},\mathbf{y};z)+G^{(0)}(\mathbf{x},\mathbf{x}_0;z)T_\Theta(\mathbf{x}_0;z)G^{(0)}(\mathbf{x}_0,\mathbf{y};z) , \tag{9}$$

where $T_\Theta(\mathbf{x}_0;z)$ corresponds to the transition matrix (T matrix) in the scattering theory and is given in terms of the unperturbed Green's function as

$$T(z)\equiv T_\Theta(\mathbf{x}_0;z) = \frac{e^{i\Theta}-1}{(i-z)\int G^{(0)}(\mathbf{x},\mathbf{x}_0;z)G^{(0)}(\mathbf{x},\mathbf{x}_0;+i)d\mathbf{x}+e^{i\Theta}(i+z)\int G^{(0)}(\mathbf{x},\mathbf{x}_0;z)G^{(0)}(\mathbf{x},\mathbf{x}_0;-i)d\mathbf{x}} . \tag{10}$$

Substituting Eq. (2) into Eq. (10) yields the T matrix

$$T(z)=[v_B^{-1}-\bar{G}(z)]^{-1} , \tag{11}$$

where

$$v_B^{-1}\equiv(v_B(\mathbf{x}_0;\Theta))^{-1}=\frac{\sin\Theta}{1-\cos\Theta}\sum_{n=1}^{\infty}\frac{(\varphi_n(\mathbf{x}_0))^2}{E_n^2+1} , \tag{12}$$

$$\bar{G}(z)\equiv\bar{G}(\mathbf{x}_0;z)=\sum_{n=1}^{\infty}(\varphi_n(\mathbf{x}_0))^2\left[\frac{1}{z-E_n}+\frac{E_n}{E_n^2+1}\right] . \tag{13}$$

Note that v_B ranges over all real numbers as $0\le\Theta<2\pi$. A perturbed system can be uniquely specified by assigning a real number v_B (and the position $\mathbf{x}_0$ of the scatterer). In this sense, v_B might be considered as a coupling constant of the scatterer. We will hereafter refer to v_B as the *bare coupling constant.*

We can realize from Eq. (11) that the eigenvalue problem of the perturbed singular system is reduced to finding all roots of the transcendental equation

$$\bar{G}(z)=v_B^{-1} . \tag{14}$$

Figure 1 shows a schematic graph of $\bar{G}(z)$. It can be seen that because $\bar{G}(z)$ is a monotonously decreasing function of z between two unperturbed energies, each solution of Eq. (14) is isolated between them. It should also be noted that $\bar{G}(z)$ has just one inflection point between two unperturbed energies. The physical meaning of the inflection points of $\bar{G}(z)$ will be discussed in detail later in this paper.

The eigenfunction $\psi_n(\mathbf{x})$ with eigenvalue $z=z_n$, which is the nth root of Eq. (14), is obtained by analyzing the residue of the corresponding pole of the Green's function

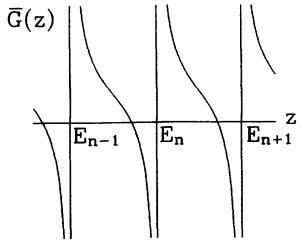

FIG. 1. Schematic graph of $\bar{G}(z)$ in Eq. (13).

of Eq. (9):

$$\psi_n(\mathbf{x})=N_nG^{(0)}(\mathbf{x},\mathbf{x}_0;z_n) , \tag{15}$$

where the normalization factor N_n is determined by

$$N_n^{-2}=\sum_{l=1}^{\infty}\frac{(\varphi_l(\mathbf{x}_0))^2}{(z_n-E_l)^2} . \tag{16}$$

III. BARE VERSUS PHYSICAL COUPLING CONSTANTS OF THE SCATTERER

In the preceding section the bare coupling constant of the scatterer, v_B, has been defined by following self-adjoint extension theory. The physical meaning of v_B is, however, not clear at this stage. It will be shown in this section that v_B should not be considered as a direct measure of the strength of the scatterer from the physical point of view. In order to obtain such a measure, we will introduce another coupling constant and make clear the relation between the two coupling constants.

In order to clarify the reason for introducing another coupling constant of the scatterer, we begin by examining a one-dimensional billiard problem with a pointlike scatterer, which we frequently come across in standard textbooks of quantum mechanics. Not only is this easy to handle but it also has the merit that we know from the start how to define a coupling constant which directly represents the strength of the scatterer. In addition, it serves to make clear the relation between the two coupling constants.

Suppose that a pointlike particle with mass $M=\frac{1}{2}$ is moving in a one-dimensional billiard with length $l=\pi$. The Hamiltonian of this system is

$$H_0=-\frac{d^2}{dx^2}+V(x) , \tag{17}$$

where the potential is given by

$$V(x)=\begin{cases}0 , & 0\le x\le\pi\\ \infty & \text{otherwise} .\end{cases} \tag{18}$$

The eigenvalues E_n and the corresponding eigenfunctions $\varphi_n(x)$ ($n=1,2,3,\ldots$) of H_0 are given by

$$E_n=n^2 , \tag{19}$$

and

$$\varphi_n(x)=\sqrt{(2/\pi)}\sin nx \ , \tag{20}$$

respectively. Let us attach a pointlike obstacle to the billiard. To avoid numerical complexity, the position of the obstacle is supposed to be the center of the billiard $[x_0=(\pi/2)]$. In this case, the stationary Schrödinger equation is written as

$$\left[H_0+v_P\delta\left[x-\frac{\pi}{2}\right]\right]\psi(x)=z\psi(x) \ , \tag{21}$$

where z and $\psi(x)$ are an eigenvalue and a corresponding eigenfunction of the perturbed system, respectively. The value of a real number v_P in Eq. (21) can be considered as a measure of the physical strength of the scatterer as we might naturally expect.

The integration of Eq. (21) over an infinitesimal range which includes the position of the obstacle, $x_0=(\pi/2)$, leads to

$$\lim_{\eta\searrow 0}\left[\psi'\left[\frac{\pi}{2}+\eta\right]-\psi'\left[\frac{\pi}{2}-\eta\right]\right]=v_P\psi\left[\frac{\pi}{2}\right] . \tag{22}$$

It is a well-known fact that the jump of the derivative of the wave function at the pointlike obstacle is proportional to v_P. Because the system has a reflection symmetry $(x\leftrightarrow\pi-x)$, we can assume the wave function in the left half as

$$\psi(x)=c\sin kx \quad \left[0\le x\le\frac{\pi}{2}\right] , \tag{23}$$

and in the right half as

$$\psi(x)=c\sin k(\pi-x) \quad \left[\frac{\pi}{2}<x\le\pi\right] , \tag{24}$$

where c is a normalization constant. [The continuity of the wave function at $x_0=(\pi/2)$ has already been taken into account by employing the same normalization constant in Eqs. (23) and (24).] Using the condition of Eq. (22), we can obtain the following equation, which determines the perturbed eigenvalue $z=k^2$:

$$-\frac{1}{2k}\tan\frac{k\pi}{2}=v_P^{-1} . \tag{25}$$

With the aid of

$$-\frac{\pi}{4x}\tan\frac{\pi x}{2}=\sum_{n=1}^{\infty}\frac{1}{x^2-(2n-1)^2} , \tag{26}$$

and using $(\varphi_{2n-1}(\pi/2))^2=(2/\pi)$ and $E_{2n-1}=(2n-1)^2$, we can rewrite Eq. (25) as

$$\sum_{n=1}^{\infty}\frac{(\varphi_{2n-1}(\pi/2))^2}{z-E_{2n-1}}=v_P^{-1} . \tag{27}$$

Note that, because we have located the obstacle at the center of the billiard, it affects only even parity unperturbed eigenstates [$\varphi_n(x)$ with odd n].

On the other hand, if we apply the formalism in the preceding section to this simple system, we can obtain

$$\sum_{n=1}^{\infty}(\varphi_{2n-1}(\pi/2))^2\left[\frac{1}{z-E_{2n-1}}+\frac{E_{2n-1}}{E_{2n-1}^2+1}\right]=v_B^{-1} . \tag{28}$$

[See Eqs. (13) and (14).] A direct comparison with Eq. (27) and Eq. (28) tells us that v_B differs from v_P and indeed yields

$$v_P^{-1}=v_B^{-1}-\sum_{n=1}^{\infty}(\varphi_{2n-1}(\pi/2))^2\frac{E_{2n-1}}{E_{2n-1}^2+1} . \tag{29}$$

A lesson which we obtain from the one-dimensional billiard problem just discussed is summarized as follows. First, the bare coupling constant v_B introduced in the preceding section can never be a direct measure of the strength of the pointlike scatterer. Second, we can realize a prescription for how to define, in terms of v_B, a coupling constant which directly represents the strength of the scatterer: we should *define* such a coupling constant by

$$v_P^{-1}\equiv v_B^{-1}-\sum_{n=1}^{\infty}(\varphi_n(\mathbf{x}_0))^2\frac{E_n}{E_n^2+1} . \tag{30}$$

In the following argument, we will refer to v_P defined by Eq. (30) as the *physical coupling constant.* In terms of v_P, the T matrix of Eq. (11) is rewritten as

$$T(z)=[v_P^{-1}-G^{(0)}(\mathbf{x}_0,\mathbf{x}_0;z)]^{-1} . \tag{31}$$

The physical meaning of Eq. (31) is clearly seen by expanding the right-hand side (rhs) in a Taylor series,

$$T(z)=v_P\sum_{n=0}^{\infty}(G^{(0)}(\mathbf{x}_0,\mathbf{x}_0;z)v_P)^n . \tag{32}$$

Considering that the Green's function $G^{(0)}(\mathbf{x},\mathbf{y};z)$ represents a particle propagation from $\mathbf{x}$ to $\mathbf{y}$, we realize that the T matrix of Eq. (32) represents a sum of multiple scatterings by the pointlike obstacle with the coupling constant v_P. This also justifies our identification of v_P with the physical strength of the scatterer.

It is important to notice that the above discussion has one subtle problem concerning the convergence of an infinite series. The infinite series on the rhs of Eq. (30) converges if and only if $\alpha<0$ in Eq. (8). (In case of the one-dimensional billiard problem, $\alpha=-\frac{1}{2}$. Hence, the infinite series converges.) Therefore the definition of the physical coupling constant v_P in Eq. (30) is justified if and only if $\alpha<0$. In this case, the difference between the inverses of the bare and physical coupling constants is nothing but the limit of the infinite series, which is a certain constant value independent of energy z. For $0\le\alpha<1$, however, the definition of the physical coupling constant in Eq. (30) loses its meaning. Thus, we are forced to deal with v_B explicitly. Then how should we recognize the strength of the scatterer in the physical sense?

In order to clarify essential points for $0\le\alpha<1$, we first notice the fact that although each of the two terms on the rhs of Eq. (13) diverges when summed separately, the sum of the two together converges into a finite value (at fixed $z\neq E_n$). Therefore, even if we restrict the infinite

series within a finite number of terms, say $n_{\max}$, the error induced in $\bar{G}(z)$ can be controlled within an arbitrary accuracy by taking $n_{\max}$ as sufficiently large. Keeping in mind that any physical essence must never be lost, we begin by making an estimate of the upper bound on the allowable error in $\bar{G}(z)$.

It is obvious from Eq. (15) that if a perturbed energy eigenvalue is close to an unperturbed energy eigenvalue then the corresponding perturbed eigenfunction is not appreciably different from the corresponding unperturbed eigenfunction. This is because the Green's function on the rhs of Eq. (15) can be approximated by a single term which has a pole at the unperturbed energy and the residue of which is proportional to the unperturbed eigenfunction. This indicates that disturbance by the obstacle could be visualized only for the eigenstates having an eigenvalue z_n such that $\bar{G}(z)$ has an inflection point in the vicinity of the eigenvalue z_n (see Fig. 1). This gives us a criterion for an estimate of the upper bound on the error in $\bar{G}(z)$: we can allow the error involved in approximating $\bar{G}(z)$ by a finite summation to the extent that it does not essentially change $\bar{G}(z)$ in the vicinity of the inflection points. This means that the magnitude of the allowable error in $\bar{G}(z)$ should be appreciably smaller than $\langle|\bar{G}'(\tilde{z})|\rangle\rho_{\rm av}^{-1}$, the product of the average absolute value of the derivative of $\bar{G}(z)$ at the inflection points $\tilde{z}$ and the mean level spacing. Here, the average $\langle\ \rangle$ is taken over the energy region under consideration. Let us make an estimate of the product just mentioned. Assume that $\rho_{\rm av}$ can be considered as constant in the energy region. Replacing $(\varphi_n(\mathbf{x}_0))^2$ in $\bar{G}(z)$ by the average value and assuming that the inflection points of $\bar{G}(z)$ appear at the midpoint between two neighboring unperturbed energies, we can loosely estimate

$$\langle|\bar{G}'(\tilde{z})|\rangle\rho_{\rm av}^{-1}\sim\langle(\varphi_n(\mathbf{x}_0))^2\rangle\sum_{n=1}^{\infty}\frac{2}{\{(n-\frac{1}{2})\rho_{\rm av}^{-1}\}^2}\rho_{\rm av}^{-1}\ . \quad (33)$$

Using

$$\sum_{n=1}^{\infty}\frac{1}{(2n-1)^2}=\frac{\pi^2}{8}\ , \quad (34)$$

we obtain

$$\langle|\bar{G}'(\tilde{z})|\rangle\rho_{\rm av}^{-1}\sim\pi^2\langle(\varphi_n(\mathbf{x}_0))^2\rangle\rho_{\rm av}\ . \quad (35)$$

The above consideration leads us to the conclusion that the upper bound on the allowable error in $\bar{G}(z)$, say ϵ, is

$$\epsilon\sim\langle(\varphi_n(\mathbf{x}_0))^2\rangle\rho_{\rm av}\ . \quad (36)$$

(This, of course, does not mean that ϵ is exactly $\langle(\varphi_n(\mathbf{x}_0))^2\rangle\rho_{\rm av}$, but that ϵ is of the order of, or approximately, $\langle(\varphi_n(\mathbf{x}_0))^2\rangle\rho_{\rm av}$.) Note that we have implicitly assumed in Eq. (33) that the average level density $\rho_{\rm av}$ is constant over the whole energy region. This is not the case in general. Nevertheless, this assumption is quite adequate because the series on the left-hand side (lhs) of Eq. (34) converges rapidly into the limit. This means that ϵ can be estimated in terms of the locally averaged quantities in the energy region under consideration.

We stress that although the physical meaning of ϵ might not necessarily be clear at this stage, it is not a mere error in $\bar{G}(z)$ and should be taken as a certain finite value as estimated above. The magnitude of ϵ can be considered to represent an extent of the allowable error in v_B^{-1}. In other words, the physics in the energy region under consideration is not distorted by changing v_B^{-1} by an extent of ϵ.

Let us proceed to the next step. We define an *effective basis* by $\{\varphi_n(\mathbf{x})\}$ $[n=1,2,3,\ldots,n_{\rm eff}(z,\epsilon)]$, where $n_{\rm eff}(z,\epsilon)$ is determined by

$$\sum_{n=n_{\rm eff}(z,\epsilon)+1}^{\infty}(\varphi_n(\mathbf{x}_0))^2\left[\frac{1}{z-E_n}+\frac{E_n}{E_n^2+1}\right]=-\epsilon\ , \quad (37)$$

or, equivalently,

$$\bar{G}(z)=\sum_{n=1}^{n_{\rm eff}(z,\epsilon)}(\varphi_n(\mathbf{x}_0))^2\left[\frac{1}{z-E_n}+\frac{E_n}{E_n^2+1}\right]-\epsilon\ . \quad (38)$$

The number of the unperturbed eigenfunctions consisting of the effective basis, $n_{\rm eff}(z,\epsilon)$, depends on the energy z as well as on the value of ϵ just introduced and can be considered to be a minimum number of the lowest unperturbed eigenstates for obtaining $\bar{G}(z)$ within the accuracy of ϵ. [Note that the terms with $n>n_{\rm eff}(z,\epsilon)$ in the infinite series of $\bar{G}(z)$ have a negative contribution.] Using Eq. (38), the transcendental equation of Eq. (14), which determines perturbed energy eigenvalues, is rewritten as

$$\sum_{n=1}^{n_{\rm eff}(z,\epsilon)}(\varphi_n(\mathbf{x}_0))^2\left[\frac{1}{z-E_n}+\frac{E_n}{E_n^2+1}\right]=v_B^{-1}+\epsilon\ . \quad (39)$$

A remarkable feature in Eq. (39) is that the summation on the lhs is not an infinite series but a finite summation. This indicates that we have finally come to the point where the same argument as for $\alpha<0$ holds for $0\le\alpha<1$: we define the physical coupling constant of the scatterer, $v_P(z)$, by

$$(v_P(z))^{-1}\equiv v_B^{-1}-\sum_{n=1}^{n_{\rm eff}(z,\epsilon)}(\varphi_n(\mathbf{x}_0))^2\frac{E_n}{E_n^2+1}+\epsilon\ , \quad (40)$$

which depends on the energy z through z explicitly as well as through ϵ implicitly. In terms of $v_P(z)$, Eq. (39) is written as

$$\sum_{n=1}^{n_{\rm eff}(z,\epsilon)}\frac{(\varphi_n(\mathbf{x}_0))^2}{z-E_n}=(v_P(z))^{-1}\ . \quad (41)$$

Immediately, we can see a similarity between Eqs. (41) and (27). Taking a limit $(v_P(z))^{-1}\to 0$, we can attain the condition for the physically strong-coupling limit in terms of the bare coupling constant v_B:

$$v_B^{-1}\sim\sum_{n=1}^{n_{\rm eff}(z,\epsilon)}(\varphi_n(\mathbf{x}_0))^2\frac{E_n}{E_n^2+1}-\epsilon\ . \quad (42)$$

Equation (42) indicates the relation which should be satisfied between v_B and z in order for the physically strong coupling to indeed occur.

One of notable physical indications of Eq. (42) is that for any positive value of v_B there exists an energy z which satisfies the condition of Eq. (42). This is because $n_{\rm eff}(z,\epsilon)$ is an increasing function of z and diverges to infinity as

$z \to \infty$ (for $0 \le \alpha < 1$). Suppose that we first set v_B to be a certain large positive value. Then the strong coupling occurs at low energy. If the value of v_B decreases adiabatically, the strong-coupling region shifts to the higher energy region and diverges to infinity as $v_B \to 0$ (as the system gradually approaches the integrable system without the scatterer). It is also understood that for a fixed positive value of v_B the physically strong coupling appears only in the energy region where Eq. (42) is fulfilled, while it never appears at the lower or higher energy.

Formally, the above consideration for $0 \le \alpha < 1$ is applicable to the case of $\alpha < 0$. The essential difference between the two cases is that although the summation on the rhs of Eq. (42) diverges as $z \to \infty$ [$n_{\rm eff}(z,\epsilon) \to \infty$] for $0 \le \alpha < 1$, it converges into a certain finite value for $\alpha < 0$. This is consistent with the fact that the value of v_P such that the physically strong coupling appears is independent of z for $\alpha < 0$ as pointed out before.

Before closing this section, we summarize the discussion for $0 \le \alpha < 1$. In this case, we have encountered in the beginning the problem concerning the divergence of an infinite series. This is because we have attempted to take into account the whole basis, $\{\varphi_n(\mathbf{x})\}$ ($n = 1,2,3,\ldots$), which includes redundant contamination shading the underlying physics. We have realized, however, that we need not assign the value of v_B^{-1} exactly as long as we do not miss the inflection points of $\bar{G}(z)$. The magnitude of ϵ is considered to be the upper bound on the allowable error in v_B^{-1} and should be determined according to the energy region under consideration. An effective basis has been introduced as a collection of necessary and sufficient lowest unperturbed eigenstates which reproduce the physics of the perturbed system in the energy region. By restricting the whole basis to the effective basis, we have succeeded not only in removing negligible contamination without losing any physical significance, but also in avoiding the divergence of the infinite series. In this way, we have obtained the condition for the physically strong coupling to appear for $0 \le \alpha < 1$.

IV. WAVE CHAOS IN RECTANGULAR BILLIARDS WITH A POINTLIKE SCATTERER

In this section, we apply the discussion in the preceding section to rectangular billiards with a single pointlike scatterer. Its validity is confirmed in numerical results. Also, statistical properties of energy eigenvalues as well as wave functions are examined in order to see whether or not wave chaos appears under the condition expected from the general argument. Furthermore, some previous papers are reviewed from the renewed viewpoint.

The Hamiltonian of a rectangular billiard with side lengths l_x and l_y is given by

$$H_0 = -\frac{1}{2M}\left[\frac{\partial^2}{\partial x^2}+\frac{\partial^2}{\partial y^2}\right]+V(x,y)\ , \tag{43}$$

where the potential is

$$V(x,y)=\begin{cases}0, & 0 \le x \le l_x, 0 \le y \le l_y \\ \infty & \text{otherwise}\ .\end{cases} \tag{44}$$

By solving the stationary Schrödinger equation for H_0 with the Dirichlet boundary condition that wave functions vanish on the boundary, we can straightforwardly show that the eigenvalues E_{n_x,n_y} and the corresponding eigenfunctions $\varphi_{n_x,n_y}(x,y)$ ($n_x,n_y = 1,2,3.\ldots$) of H_0 are

$$E_{n_x,n_y}=\frac{1}{2M}\left\{\left[\frac{n_x\pi}{l_x}\right]^2+\left[\frac{n_y\pi}{l_y}\right]^2\right\} \tag{45}$$

and

$$\varphi_{n_x,n_y}(x,y)=\left[\frac{4}{l_x l_y}\right]^{1/2}\sin\frac{n_x\pi x}{l_x}\sin\frac{n_y\pi y}{l_y}\ , \tag{46}$$

respectively. We set the mass $M = 8\pi$ and the side lengths $l_x = (\pi/3)$ and $l_y = (3/\pi)$ in the following argument. To simplify things, we consider the case where a pointlike scatterer is located at the center of the rectangle; $\mathbf{x}_0 = [(l_x/2),(l_y/2)]$. In this parametrization, only even-even parity states (with n_x and n_y odd) are affected by the obstacle. Arranging the double-indexed eigenvalues and eigenfunctions of the even-even parity states in ascending order of magnitude of eigenvalues, E_n and $\varphi_n(x,y)$ ($n = 2,3,\ldots$), we obtain

$$\bar{G}(z)=4\sum_{n=1}^{\infty}\left[\frac{1}{z-E_n}+\frac{E_n}{E_n^2+1}\right]\ , \tag{47}$$

because $(\varphi_n(\mathbf{x}_0))^2 = 4$ for any n. The average level density of the even-even parity states are given by $\rho_{\rm av}(E) \sim 1$ following the Weyl formula. This means $E_n \sim n$. Note that $\alpha = 0$ for two-dimensional billiards. Therefore, we cannot define the physical coupling constant v_P in a trivial manner [as in Eq. (30)]. In the following numerical treatment, we take 100 000 lowest even-even parity states, which is enough to obtain sufficient convergence in energy regions under consideration.

Let us begin by finding the condition for the physically strong coupling following the consideration in the previous section. It should be described in terms of the bare coupling constant v_B. We first notice that the upper bound on the allowable error in $\bar{G}(z)$ (equivalently in v_B^{-1}), ϵ, is of the order of one, independently of z. Indeed we can estimate $\epsilon \sim 4$ following Eq. (36), because $(\varphi_n(\mathbf{x}_0))^2 = 4$ and $\rho_{\rm av} \sim 1$. (That the value of ϵ is 4 is due to our specific geometrical choice to put the scatterer in the center of the rectangle. On the other hand, the energy-independence of ϵ is valid for any $\mathbf{x}_0$. Indeed we will see later in this paper that the amplitude distribution $P(\psi)$ takes the same form for any φ_n except small n.) Hereafter we set $\epsilon = 1$, which justifies the following estimate of the number of the unperturbed eigenfunctions consisting of the effective basis, $n_{\rm eff}(z,\epsilon)$. By following Eq. (37), $n_{\rm eff}(z,\epsilon)$ is determined by

$$4\sum_{n=n_{\rm eff}(z,\epsilon)+1}^{\infty}\left[\frac{1}{z-E_n}+\frac{E_n}{E_n^2+1}\right]=-\epsilon\ . \tag{48}$$

Here, let us replace the summation by an integral on the lhs of Eq. (48). Then, because $\rho_{\rm av}(E)\sim 1$ and hence $E_n\sim n$,

$$4\int_{n_{\rm eff}(z,\epsilon)}^{\infty}\left[\frac{1}{z-E}+\frac{E}{E^2+1}\right]dE\sim-\epsilon\ . \tag{49}$$

Here, we set

$$F(z,E)\equiv F_1(z,E)+F_2(E)\ , \tag{50}$$

$$F_1(z,E)\equiv\int\frac{1}{z-E}dE=-\ln|z-E|\ , \tag{51}$$

$$F_2(E)\equiv\int\frac{E}{E^2+1}dE=\tfrac{1}{2}\ln(E^2+1)\ . \tag{52}$$

If $1<z<E$ then

$$F_1(z,E)=-\ln E+\frac{z}{E}+\frac{1}{2}\left[\frac{z}{E}\right]^2+\ldots\ , \tag{53}$$

$$F_2(E)=\ln E+\frac{1}{E^2}-\ldots\ , \tag{54}$$

holds. Hence

$$F(z,E)=\frac{z}{E}+\ldots\ . \tag{55}$$

Note that the logarithmic terms in $F_1(z,E)$ and $F_2(E)$ cancel each other in $F(z,E)$. Equation (55) indicates that Eq. (49) becomes

$$\frac{4z}{n_{\rm eff}(z,\epsilon)}\sim\epsilon\ . \tag{56}$$

Thus, the approximate estimate of $n_{\rm eff}(z,\epsilon)$ is given by

$$n_{\rm eff}(z,\epsilon)\sim\frac{4z}{\epsilon}\ . \tag{57}$$

By following Eq. (42), the condition for the physically strong coupling is determined by

$$v_B^{-1}\sim 4\int_0^{n_{\rm eff}(z,\epsilon)}\frac{E}{E^2+1}dE-\epsilon\ . \tag{58}$$

(Here we have replaced the summation by an integral on the rhs as before.) Equations (52) and (54) indicate that Eq. (58) can be written as

$$v_B^{-1}\sim 4\ln n_{\rm eff}(z,\epsilon)-\epsilon\ . \tag{59}$$

Keeping Eq. (57) and $\epsilon=1$ in mind and ignoring the redundant constant on the rhs of Eq. (59), we finally realize the condition for the physically strong coupling in a simple form:

$$v_B^{-1}\sim 4\ln z\ . \tag{60}$$

Let us proceed to check the validity of the present argument in the numerical calculation. In Fig. 2, we show $\bar{G}(z)$ in three different energy regions. Our first observation is that the estimate of the order of the magnitude of ϵ (~ 1) is quite satisfactory: this "resolution" is adequate to "see" the inflection points of $\bar{G}(z)$ in the horizontal direction. We also recognize the energy independence of ϵ. This is because the average of the derivative of $\bar{G}(z)$ at the inflection points as well as the average level density are independent of the energy. The broken line in Fig. 2 shows the values of $4\ln z$ in Eq. (60). It is noteworthy that the inflection points of $\bar{G}(z)$ actually appear along this curve. In order to see the physical importance of the inflection points of $\bar{G}(z)$, we show a "transition" of a perturbed wave function along $\bar{G}(z)$ in Fig. 3. Figures

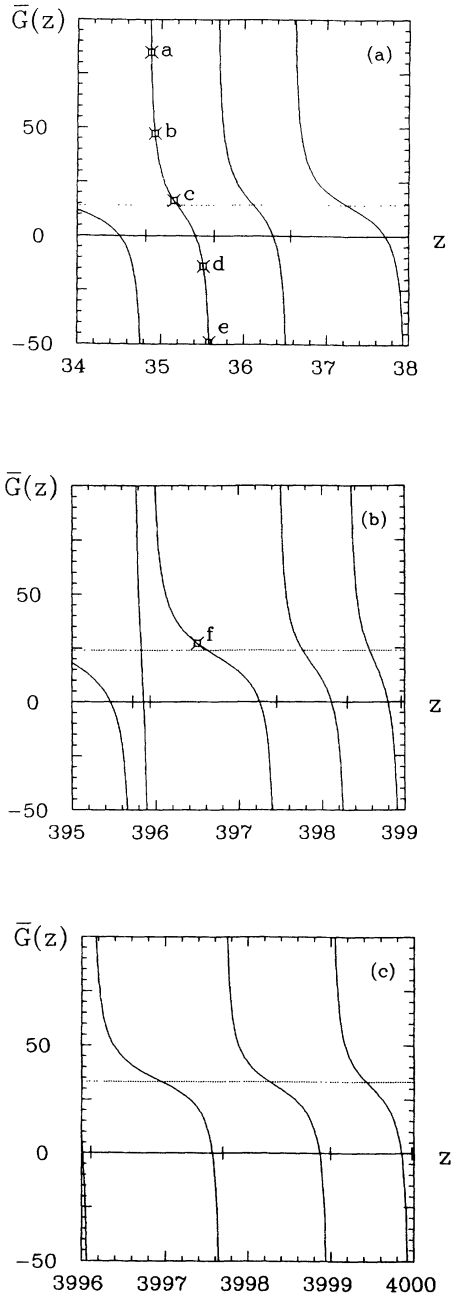

FIG. 2. Behavior of $\bar{G}(z)$ in three different energy regions. Unperturbed energies are indicated by vertical lines on the z axis. The broken line is a plot of $4\ln z$. In (a), the coordinates of the points indicated by a, b, c, d, and e are $(z,\bar{G}(z))=(34.88,84.84)$, $(34.93,47.24)$, $(35.16,16.31)$, $(35.51,-14.11)$, and $(35.58,-49.11)$, respectively. In (b), the coordinates of the point indicated by f are $(z,\bar{G}(z))=(396.50,27.25)$.

3(a)–3(e) correspond to the wave function for the eigenstates indicated by $a-e$, respectively, in Fig. 2(a). Each is considered as the eigenfunction with an eigenvalue z for the system with $v_B^{-1}=\bar{G}(z)$. From Fig. 3, it can be confirmed that the mixture of the unperturbed eigenfunctions actually emerges in the vicinity of the inflection points of $\bar{G}(z)$, while the wave function does not differ substantially from one of the unperturbed eigenfunctions in the region far from the inflection points.

The theoretical and numerical considerations just made convince us that the condition of Eq. (60) is indispensable for the appearance of wave chaos in our singular rectangular billiard.

We now stand at the point where we start to investigate statistical properties of the quantum spectrum including energy eigenvalues and wave functions, which tell us whether or not wave chaos indeed appears in rectangular billiards with a single pointlike scatterer. We begin by examining the amplitude distribution $P(\psi)$ [23], which corresponds to the probability of finding a value of wave function. For quantized classically chaotic billiards with area S, there is a conjecture [23,24] that the proba-

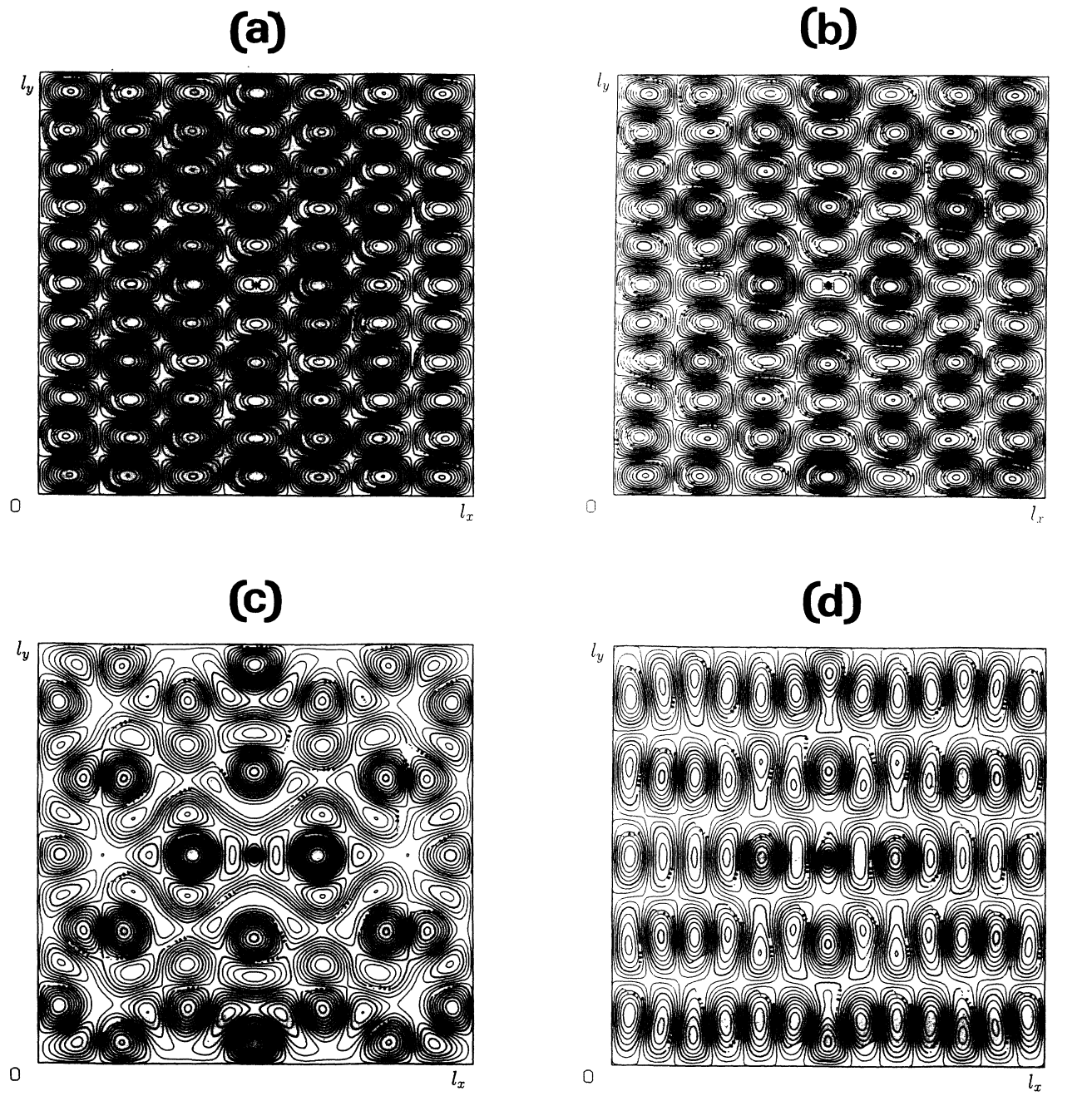

FIG. 3. The contour plot of the wave function for the eigenstates indicated by $a-e$ in Fig. 2(a) and f in Fig. 2(b) is shown in (a)–(f), respectively. Each wave function corresponds to the eigenfunction with an energy eigenvalue z for the system with $v_B^{-1}=\bar{G}(z)$. A pointlike scatterer is located at the center of the billiard.

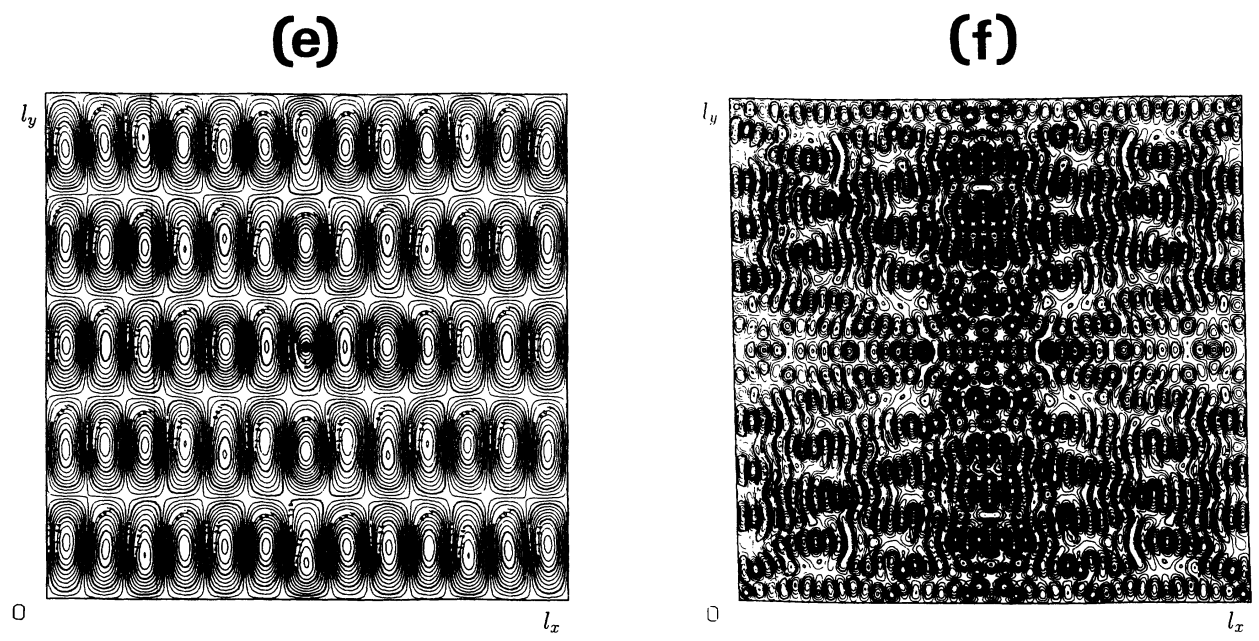

FIG. 3. (*Continued*).

bility is given by

$$P(\psi)=\left[\frac{S}{2\pi}\right]^{1/2} e^{-(s\psi^2/2)} . \tag{61}$$

This might be expected to appear in the physically strong-coupling region in our case. On the other hand, the following assertion is valid in the weak-coupling limit for rectangular billiards, where ψ is one of the unperturbed eigenfunctions $\{\varphi_{n_x,n_y}\}$ in Eq. (46): if we restrict the domain of ψ to a rectangular subdomain, enclosed by nodal lines, on which ψ is positive, then $P(\psi)$ is given by

$$P(\psi)=\begin{cases}\bar{P}(\psi)\equiv\dfrac{8\sqrt{S}}{\pi^2(2+\sqrt{S}\,\psi)}K\left[\dfrac{2-\sqrt{S}\,\psi}{2+\sqrt{S}\,\psi}\right], & 0<\psi\le\sqrt{(4/S)}\\ 0, \quad 4>\sqrt{(4/S)}\ , \end{cases} \tag{62}$$

where $S=l_x l_y$ and $K(k)$ is a complete elliptic integral of the first kind,

$$K(k)=\int_0^{\pi/2}\frac{d\theta}{\sqrt{1-k^2\sin^2\theta}} . \tag{63}$$

[Note that Eq. (62) is independent of the values of n_x and n_y.] Equation (62) is verified as follows. First, we consider a one-dimensional case. Let ψ be one of

$$\varphi_n(x)=\sqrt{(2/l)}\sin\frac{n\pi x}{l} \tag{64}$$

($n=1,2,3,\ldots$). In this case, it is easily shown that if the domain of ψ is restricted to segments on which ψ is positive, then the amplitude distribution is given by

$$P_1(l;\psi)=\begin{cases}\dfrac{2}{\pi}\left[\dfrac{l}{2-l\psi^2}\right]^{1/2}, & 0\le\psi<\sqrt{(2/l)}\\ 0, \quad \psi>\sqrt{(2/l)}\ . \end{cases} \tag{65}$$

(The result is independent of the value of n.) If ψ is one of $\{\varphi_{n_x,n_y}\}$ in Eq. (46) and its domain is restricted to the aforementioned rectangular subdomain, then $P(\psi)$ can be written as

$$P(\psi)=\int_0^\infty\int_0^\infty\delta(\psi-\varphi_x\varphi_y)P_1(l_x;\varphi_x)P_1(l_y;\varphi_y)d\varphi_x d\varphi_y . \tag{66}$$

Substituting Eq. (65) into the rhs of Eq. (66) and evaluating the integral lead us to Eq. (62). Equation (62) indicates that if we ignore the fact that, for n_x and n_y odd, the total domain of $\psi=\varphi_{n_x,n_y}$ (just inside the rectangle) has one more (or less) rectangular subdomains with positive ψ than those with negative ψ (which is justified for n_x and n_y large), then $P(\psi)$ on the whole rectangle can be expressed as follows:

$$P(\psi)=\begin{cases}\frac{1}{2}\bar{P}(|\psi|), & 0<|\psi|\le\sqrt{(4/S)}\\ 0, \quad |\psi|>\sqrt{(4/S)}\ . \end{cases} \tag{67}$$

Our numerical result of $P(\psi)$ is shown in Fig. 4. Similar-

ly, as before, Figs. 4(a)–4(e) correspond to the case of eigenstates indicated by $a-e$, respectively, in Fig. 2(a). The solid line corresponds to the strong-coupling limit in Eq. (61), while the broken line corresponds to the weak-coupling limit in Eq. (67). It can be seen from Fig. 4 that a Gaussian-like shape appears in $P(\psi)$ in the vicinity of the inflection point of $\bar{G}(z)$, while on departing from it such a shape tends to disappear, returning to a shape like Eq. (67). In Fig. 4(c), an asymmetric structure unlike a Gaussian curve is observed. We sometimes come across such a structure for small energy. As the energy increases, however, this asymmetry tends to disappear as shown in Fig. 4(f). This corresponds to the case of the point f in Fig. 2(b), the location of which is also in the vicinity of an inflection point of $\bar{G}(z)$. Figure 3(f) shows the corresponding wave function, which again exhibits a complicated pattern as expected.

We now proceed to examine the level statistics of our singular billiard. Figure 5 shows the nearest-neighbor level spacing distribution $P(S)$ for various values of v_B^{-1}. The statistics are taken within the eigenvalues between z_{1000} and z_{4000} in all cases. Also, the spectral rigidity $\Delta_3(L)$ is shown in Fig. 6 for the same values of v_B^{-1} as for $P(S)$. The average is taken over the same energy region as for $P(S)$. It is observed from Figs. 5 and 6 that as the value of v_B^{-1} increases from 0 to 30, the level statistics

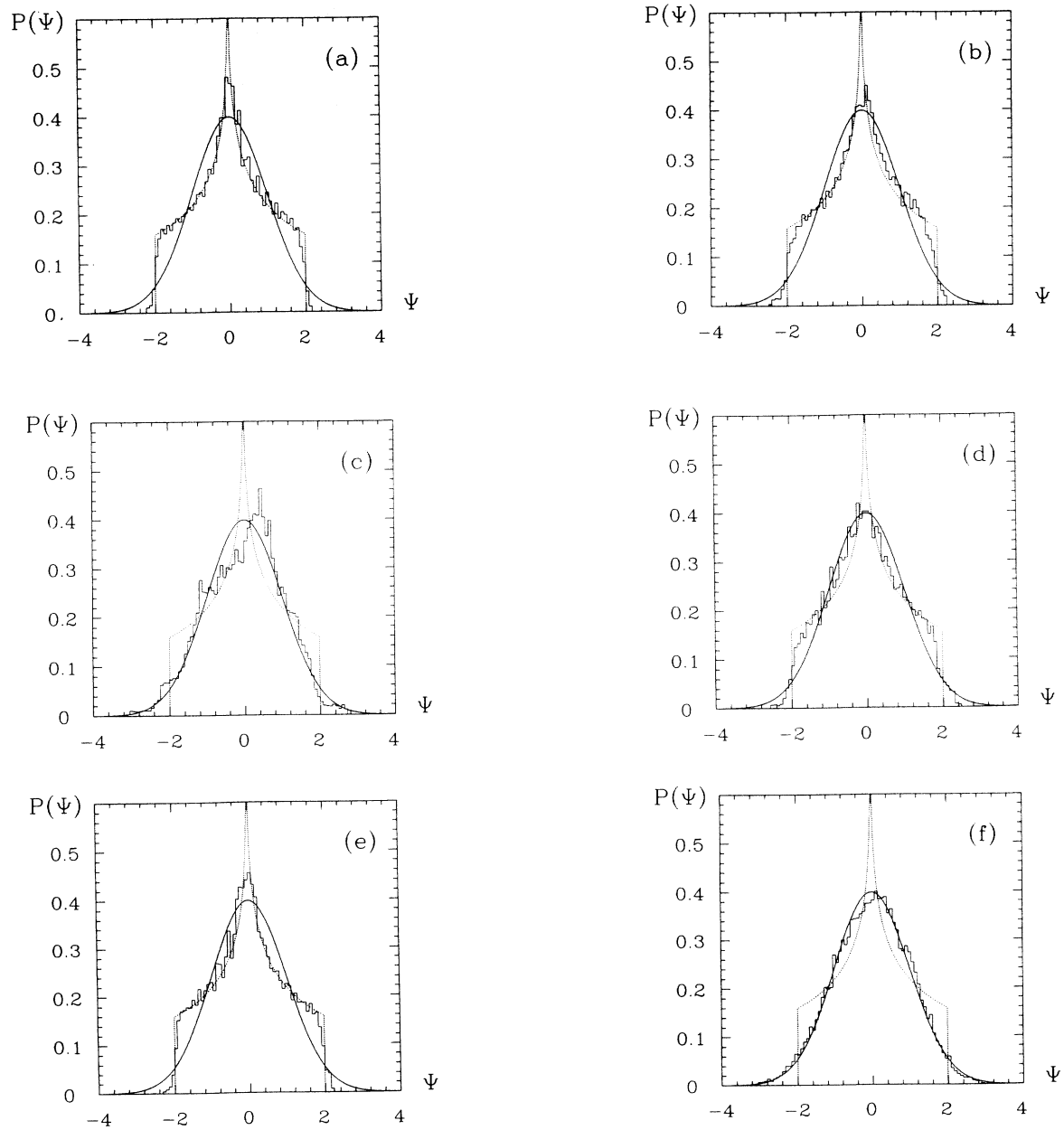

FIG. 4. The amplitude distribution $P(\psi)$ for the eigenstates indicated by $a-e$ in Fig. 2(a) and f in Fig. 2(b) is shown in (a)–(f), respectively. The solid line is $P(\psi)$ for the strong-coupling limit in Eq. (61), while the broken line is $P(\psi)$ for the weak-coupling limit in Eq. (67).

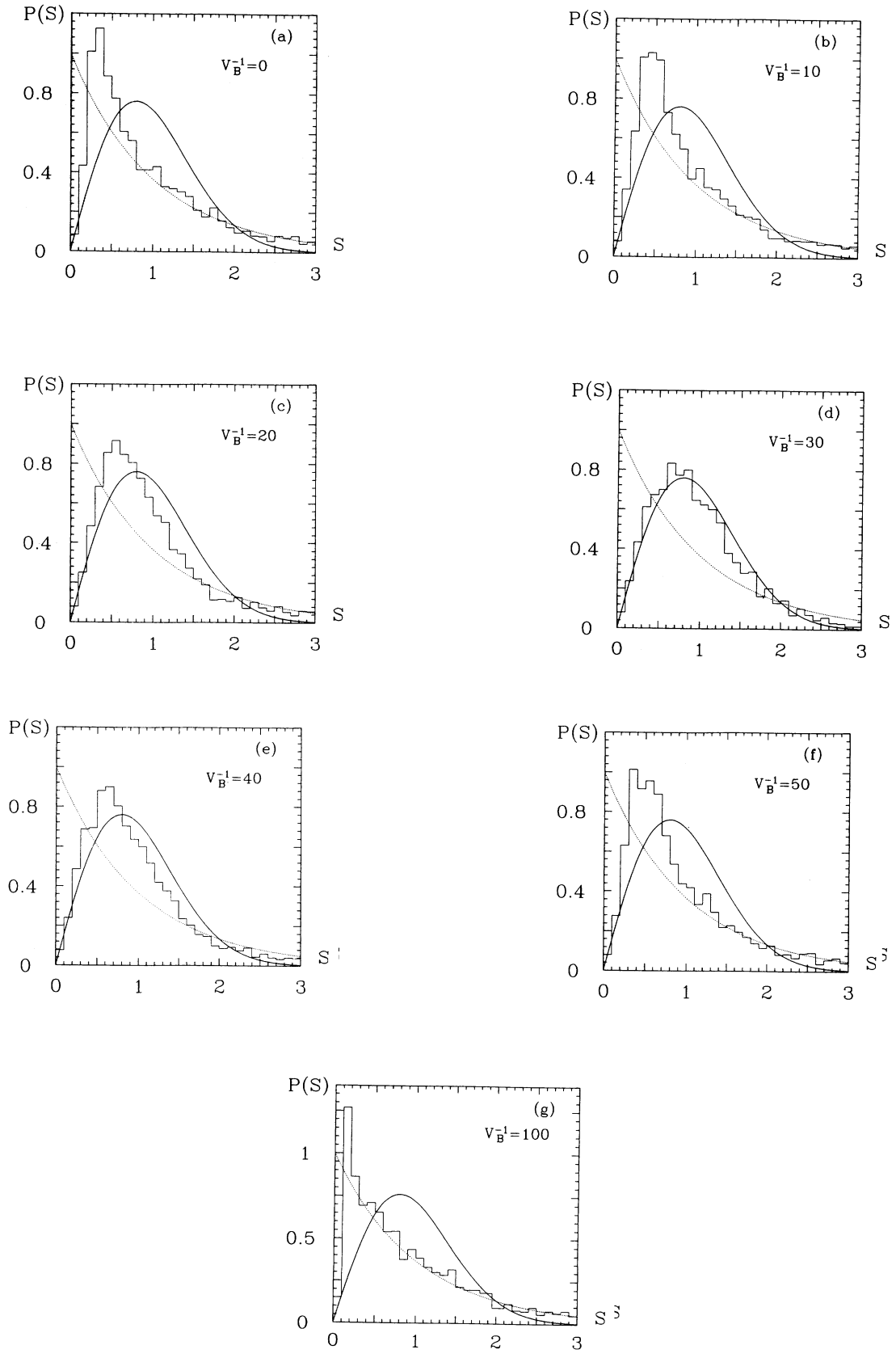

FIG. 5. The nearest-neighbor level spacing distribution $P(S)$ is shown for $v_B^{-1}=0$, 10, 20, 30, 40, 50, and 100. The statistics are taken within the eigenvalues between z_{1000} and z_{4000} in all cases. The solid (broken) line is the Wigner (Poisson) distribution.

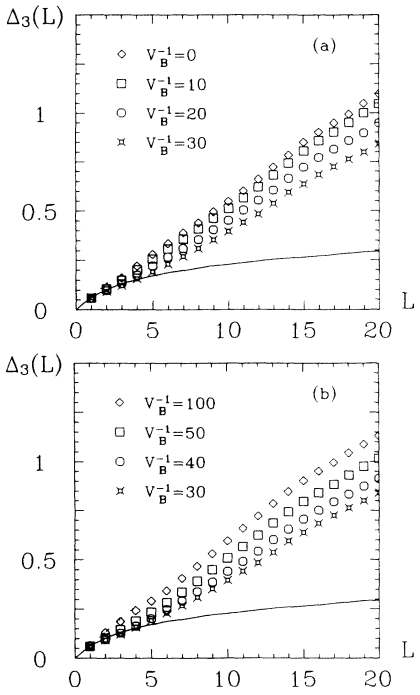

FIG. 6. The spectral rigidity $\Delta_3(L)$ is shown for $v_B^{-1}=0$, 10, 20, and 30 in (a) and for $v_B^{-1}=30$, 40, 50, and 100 in (b). The average is taken over the energy region between z_{1000} and z_{4000} in all cases. The solid (broken) line is the prediction of GOE (Poisson) statistics.

tend to approach GOE predictions, although there still remains a considerable difference in $\Delta_3(L)$ even for $v_B^{-1}=30$. On the other hand, a further increase of the value of v_B^{-1} beyond 30 leads the level statistics to the recurrence of Poisson statistics. Such dependence of the level statistics on v_B^{-1} can be well understood by noting $z_n \sim E_n \sim n$ and 4 ln 1000 = 27.631, 4 ln 4000 = 33.176 [see Fig. 2(c)]. This indicates that the physically strong coupling is attained for $v_B^{-1} \sim 30$ in this energy region. We make a closer examination of the energy dependence of the strong-coupling region by dividing the energy region into several narrow pieces. In Table I, the values of $\Delta_3(L)$ at $L=20$ in various energy regions are shown for several values of v_B^{-1}. For each line, the average is taken over the energy region between $z_{n_{\min}}$ and $z_{n_{\max}}$, where the range of n ($n_{\min} \le n \le n_{\max}$) is indicated in the first column. In view of the previous discussion, we can expect the "4 ln z dependence" of the physically strong-coupling region. Table I shows that this is in fact the case. In each line, the italic number is the minimum value and hence the closest to the value of GOE statistics. We can clearly see that the physically strong coupling is attained along the logarithmic curve. For a fixed value of v_B^{-1}, the variation of the values of $\Delta_3(L)$ is not smooth but rather fluctuating as the energy varies. This is because the values of $\Delta_3(L)$ for the unperturbed system do fluctuate as the energy varies. Its tracks can be observed for the case of $v_B^{-1}=100$, which is expected to

TABLE I. The values of $\Delta_3(L)$ at $L=20$ for $v_B^{-1}=0$, 10, 20, 25, 30, 35, 40, 50, and 100. For each line the average is taken over the energy region between $z_{n_{\min}}$ and $z_{n_{\max}}$, where the range of n ($n_{\min} \le n \le n_{\max}$) is indicated in the first column. The italic number is the minimum value in each line.

n/v_B^{-1}	0	10	20	25	30	35	40	50	100
100–300	0.936	0.832	*0.721*	0.750	0.817	0.879	0.929	0.988	1.060
300–500	1.154	1.064	0.925	*0.903*	0.940	1.008	1.077	1.155	1.249
500–700	0.886	0.825	0.716	*0.684*	0.702	0.755	0.810	0.879	0.953
700–900	1.203	1.137	1.011	*0.959*	0.961	1.023	1.090	1.179	1.275
900–1100	0.771	0.724	0.628	*0.584*	*0.584*	0.629	0.682	0.750	0.821
1100–1300	1.317	1.247	1.111	1.041	*1.030*	1.088	1.171	1.277	1.394
1300–1500	1.030	0.970	0.864	0.810	*0.797*	0.850	0.914	1.004	1.096
1500–1700	1.073	1.015	0.902	0.828	*0.794*	0.827	0.892	0.995	1.107
1700–1900	1.252	1.200	1.090	1.030	*1.012*	1.041	1.105	1.214	1.336
1900–2100	1.149	1.100	0.998	0.931	*0.902*	0.930	0.998	1.100	1.205
2100–2300	1.087	1.030	0.932	0.869	*0.834*	0.860	0.929	1.035	1.146
2300–2500	1.020	0.973	0.890	0.824	*0.782*	0.792	0.845	0.946	1.057
2500–2700	1.077	1.026	0.939	0.879	*0.843*	0.860	0.916	1.017	1.137
2700–2900	1.527	1.471	1.361	1.289	*1.219*	1.226	1.288	1.429	1.587
2900–3100	0.936	0.895	0.812	0.753	*0.703*	0.705	0.755	0.856	0.972
3100–3300	0.889	0.851	0.777	0.726	*0.680*	0.686	0.730	0.830	0.941
3300–3500	1.108	1.060	0.981	0.921	*0.880*	0.884	0.926	1.026	1.150
3500–3700	1.065	1.022	0.928	0.863	0.810	*0.809*	0.867	0.984	1.112
3700–3900	1.112	1.063	0.976	0.908	0.849	*0.839*	0.893	1.023	1.162
3900–4100	1.004	0.958	0.871	0.806	0.753	*0.745*	0.790	0.911	1.047
4100–4300	1.265	1.221	1.136	1.068	1.005	*0.990*	1.041	1.167	1.310
4300–4500	1.182	1.141	1.049	0.984	0.926	*0.911*	0.955	1.080	1.231
4500–4700	1.355	1.305	1.209	1.130	1.060	*1.040*	1.094	1.222	1.386
4700–4900	1.747	1.698	1.591	1.508	1.436	*1.426*	1.484	1.647	1.828
4900–5100	1.338	1.295	1.211	1.145	1.083	*1.065*	1.109	1.235	1.382

resemble the unperturbed case (in the energy regions listed in Table I).

From the above results concerning the statistical properties on the quantum spectrum, we can draw the conclusion that wave chaos indeed occurs in the vicinity of the inflection points of $\bar{G}(z)$ in singular rectangular billiards with a single pointlike scatterer. Because the physically strong-coupling region has logarithmic dependence on the energy, it is expected that the signature of wave chaos can be observed for any positive value of v_B: as the value of v_B decreases to zero, the energy region where wave chaos occurs shifts to the higher energy region along the logarithmic curve.

Before closing this section, let us reexamine some previous papers from the present point of view. In Ref. [19], it has been shown that in the strong-coupling limit in the sense of $v_B^{-1}\to 0$, $P(S)$ does not become Wigner-like but still remains Poisson-like in shape. This observation is the same as in Fig. 5(a). (Actually, both calculations are the same except that the statistics are taken within slightly different energy regions.) The reason for this is easily recognized in the present context. In the limit of $v_B^{-1}\to 0$, it is only at low energy that the physically strong coupling emerges. As the energy increases, the limit of $v_B^{-1}\to 0$ tends to depart from the physically strong-coupling region.

Also, the observation in Ref. [18] can be well understood from the present viewpoint. The authors in Ref. [18] intend to examine the dynamics of the strong-coupling limit in the sense of $v_B^{-1}\to 0$ by making a truncation of the basis: in finding the lth eigenvalue $z_l(\sim l)$, $\bar{G}(z)$ is approximated by

$$\bar{G}(z)\sim 4\sum_{n=l-500}^{l+500}\left[\frac{1}{z-E_n}+\frac{E_n}{E_n^2+1}\right] . \tag{68}$$

This truncation causes an error in $\bar{G}(z)$, which is estimated to be

$$\delta\bar{G}(z)\sim 4\left[\int_0^{l-500}+\int_{l+500}^{\infty}\right]\left[\frac{1}{z-E}+\frac{E}{E^2+1}\right]dE . \tag{69}$$

This leads to

$$\delta\bar{G}(z)\sim 4[F(z,l-500)-F(z,0)-F(z,l+500)] , \tag{70}$$

where $F(z,E)$ is given in Eq. (50). This yields

$$\delta\bar{G}(z)\sim 4\ln z , \tag{71}$$

for large z. Equation (71) indicates that the strong-coupling limit in the sense of $v_B^{-1}\to 0$ in Ref. [18] precisely corresponds to the physically strong-coupling limit in the sense of $v_B^{-1}\to 4\ln z\,[(v_P(z))^{-1}\to 0]$. This is the reason why the authors in Ref. [18] have observed that $P(S)$ becomes Wigner-like in the limit of $v_B^{-1}\to 0$ [actually $(v_P(z))^{-1}\to 0$]. Their observation that this property is energy independent might confirm the validity of our present discussion: the logarithmic dependence of the strong-coupling region on the energy indeed continues in the higher energy region.

V. CONCLUSION

To conclude the paper, we summarize the general argument which tells us the necessary condition for the appearance of wave chaos in singular systems with a single pointlike scatterer.

Suppose that an autonomous bounded integrable system with the Hamiltonian H_0 is given. Let E_n and $\varphi_n(\mathbf{x})$ $(n=1,2,3,\ldots)$ be the energy eigenvalues and the eigenfunctions of H_0, respectively. Furthermore, assume that the asymptotic average level density in the high energy region is

$$\rho_{\rm av}(E)\sim E^{\alpha} .$$

Then, $\alpha<1$ is required in order to attach a pointlike scatterer to the integrable system. In this case, we can specify a perturbed system by assigning a real number v_B, which has been called the *bare coupling constant* of the scatterer in this paper. If we define

$$\bar{G}(z)=\sum_{n=1}^{\infty}(\varphi_n(\mathbf{x}_0))^2\left[\frac{1}{z-E_n}+\frac{E_n}{E_n^2+1}\right] ,$$

where the pointlike obstacle is assumed to be placed at $\mathbf{x}_0$, then the eigenvalue problem of the perturbed system is reduced to the transcendental equation,

$$\bar{G}(z)=v_B^{-1} .$$

The dynamics of the singular system is essentially different accordingly as $\alpha<0$ or $0\le\alpha<1$. For $\alpha<0$, we can define the *physical coupling constant* v_P by

$$v_P^{-1}\equiv v_B^{-1}-\sum_{n=1}^{\infty}(\varphi_n(\mathbf{x}_0))^2\frac{E_n}{E_n^2+1} ,$$

because the infinite series on the rhs converges. The necessary condition for the appearance of wave chaos is $v_P^{-1}\sim 0$, that is

$$v_B^{-1}\sim\sum_{n=1}^{\infty}(\varphi_n(\mathbf{x}_0))^2\frac{E_n}{E_n^2+1} .$$

For $0\le\alpha<1$, we cannot define the physical coupling constant explicitly, contrary to the case where $\alpha<0$. In this case, let

$$\epsilon\sim\langle(\varphi_n(\mathbf{x}_0))^2\rangle\rho_{\rm av} ,$$

where the average $\langle\ \rangle$ is taken over the energy region under consideration. We then introduce an *effective basis* by $\{\varphi_n(\mathbf{x})\}$ $[n=1,2,3,\ldots,n_{\rm eff}(z,\epsilon)]$, where $n_{\rm eff}(z,\epsilon)$ satisfies

$$\bar{G}(z)=\sum_{n=1}^{n_{\rm eff}(z,\epsilon)}(\varphi_n(\mathbf{x}_0))^2\left[\frac{1}{z-E_n}+\frac{E_n}{E_n^2+1}\right]-\epsilon .$$

The number of the unperturbed eigenfunctions consisting of the effective basis, $n_{\rm eff}(z,\epsilon)$, can be considered as a necessary and sufficient number of the lowest unperturbed eigenstates needed to reproduce the dynamics of the perturbed system in the energy region under consideration. In terms of ϵ and $n_{\rm eff}(z,\epsilon)$, the necessary condition for the appearance of wave chaos in the perturbed

system is given by

$$v_B^{-1} \sim \sum_{n=1}^{n_{\text{eff}}(z,\epsilon)} (\varphi_n(\mathbf{x}_0))^2 \frac{E_n}{E_n^2+1} - \epsilon \ .$$

This indicates that if wave chaos exists it appears in various energy regions according to the value of v_B.

Note that what we have shown in this paper is the necessary condition for the appearance of wave chaos. In general, it depends on the underlying dynamics (eigenvalues and eigenfunctions) of integrable systems whether or not wave chaos actually appear when a pointlike obstacle is added to them.

For rectangular billiards with a single pointlike scatterer, we have shown in this paper that wave chaos indeed appears under the condition mentioned above. It is expected that the signature of wave chaos can be observed for any positive value of v_B. As the value of v_B decreases to zero, the energy region where wave chaos appears shifts to the higher energy along a logarithmic curve.

Let us close the paper by making two comments. First, the assumption of the integrability of unperturbed systems is unnecessary for the general argument made in this paper. Needless to say, we should refrain from using the term of wave chaos if unperturbed systems are chaotic in themselves. Second, we have seen that there still exists an appreciable difference from GOE predictions in $\Delta_3(L)$ even for the physically strong-coupling limit. This might imply that the degree of wave chaos is not strong for rectangular billiards with a single pointlike scatterer. Our recent preliminary results show, however, that $\Delta_3(L)$ becomes closer to GOE predictions as the number of scatterers increases. This confirms our present conclusion that pointlike obstacles indeed cause wave chaos in rectangular billiards.

ACKNOWLEDGMENTS

The author would like to thank T. Cheon, N. Yoshinaga, and T. Mizusaki for several useful conversations. He also expresses his gratitude to Miss R. Tapp for her careful reading of the manuscript. Numerical computations have been performed on HITAC M-880 and S-3800 computers at the Computer Centre, the University of Tokyo.

[1] A. J. Lichtenberg and M. A. Lieberman, *Regular and Stochastic Motion,* edited by F. John, J. E. Marsden, and L. Sirovich, Applied Mathematical Sciences Vol. 38 (Springer-Verlag, New York, 1983), new revised and enlarged edition, 1992.

[2] A. M. Ozorio de Almeida, *Hamiltonian Systems: Chaos and Quantization* (Cambridge University Press, Cambridge, 1988).

[3] B. V. Chirikov, Phys. Rep. **52**, 263 (1979).

[4] G. M. Zaslavsky, Phys. Rep. **80**, 157 (1981).

[5] J. Ford and M. Ilg, Phys. Rev. A **45**, 6165 (1992).

[6] F. V. M. Izrailev, Phys. Rep. **196**, 299 (1990).

[7] M. V. Berry, Proc R. Soc. London, Ser. A **413**, 183 (1987).

[8] M. V. Berry, in *Some Quantum-to-Classical Asymptotics,* Les Houches Summer School Proceedings Session 52, edited by M.-J. Giannoni, A. Voros, and J. Zinn-Justin (North-Holland, Amsterdam, 1989), p. 251.

[9] M. L. Mehta, *Random Matrices and the Statistical Theory of Energy Levels* (Academic Press, New York, 1967), new revised and enlarged edition, 1990.

[10] O. Bohigas, in *Random Matrix Theories and Chaotic Dynamics,* Les Houches Summer School Proceedings Session 52, edited by M.-J. Giannoni, A. Voros, and J. Zinn-Justin (North-Holland, Amsterdam, 1989), p. 87.

[11] M. V. Berry and M. Tabor, Proc. R. Soc. London, Ser. A **356**, 375 (1977).

[12] A. N. Zemlyakov and A. B. Katok, Math. Notes **18**, 291 (1975).

[13] R. J. Richens and M. V. Berry, Physica D **2**, 495 (1981).

[14] K. Życzkowski, Acta Phys. Pol. B **23**, 245 (1992).

[15] T. Cheon and T. D. Cohen, Phys. Rev. Lett. **62**, 2769 (1989).

[16] A. Shudo and Y. Shimizu, Phys. Rev. E **47**, 54 (1993).

[17] J. L. Vega, T. Uzer, and J. Ford, Phys. Rev. E **48**, 3414 (1993).

[18] P. Šeba and K. Życzkowski, Phys. Rev. A **44**, 3457 (1991).

[19] T. Shigehara, N. Yoshinaga, T. Cheon, and T. Mizusaki, Phys. Rev. E **47**, R3822 (1993).

[20] J. Zorbas, J. Math. Phys. **21**, 840 (1980).

[21] S. Albeverio, F. Gesztesy, R. Høegh-Krohn, and H. Holden, *Solvable Models in Quantum Mechanics,* edited by W. Beiglböck, J. L. Birman, R. P. Geroch, E. H. Lieb, T. Regge, and W. Thirring, Texts and Monographs in Physics (Springer-Verlag, New York, 1988).

[22] S. Albeverio and P. Šeba, J. Stat. Phys. **64**, 369 (1991).

[23] S. W. McDonald and A. N. Kaufman, Phys. Rev. A **37**, 3067 (1988).

[24] P. Šeba, Phys. Rev. Lett. **64**, 1855 (1990).

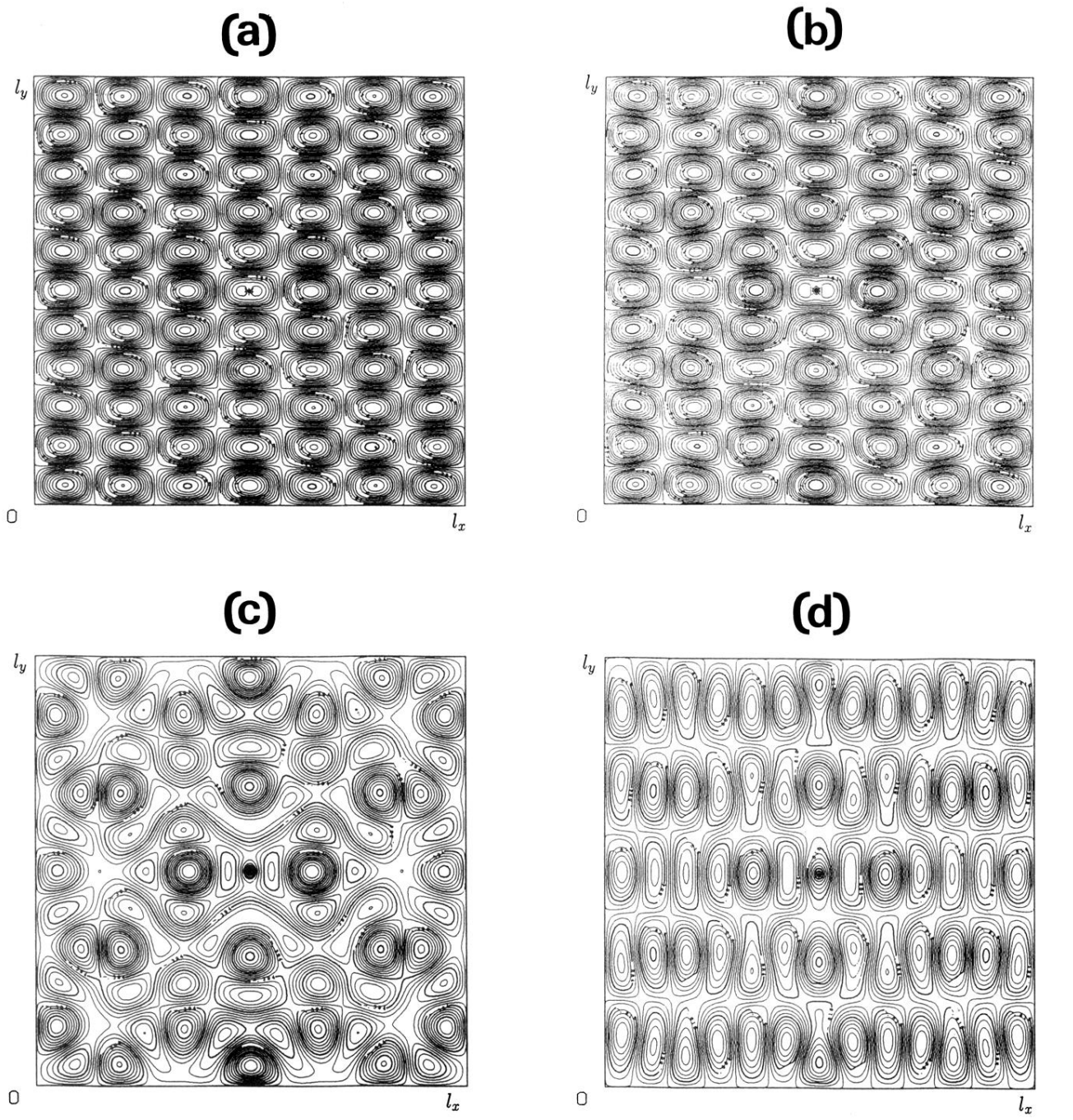

FIG. 3. The contour plot of the wave function for the eigenstates indicated by $a-e$ in Fig. 2(a) and f in Fig. 2(b) is shown in (a)–(f), respectively. Each wave function corresponds to the eigenfunction with an energy eigenvalue z for the system with $v_B^{-1}=\bar{G}(z)$. A pointlike scatterer is located at the center of the billiard.

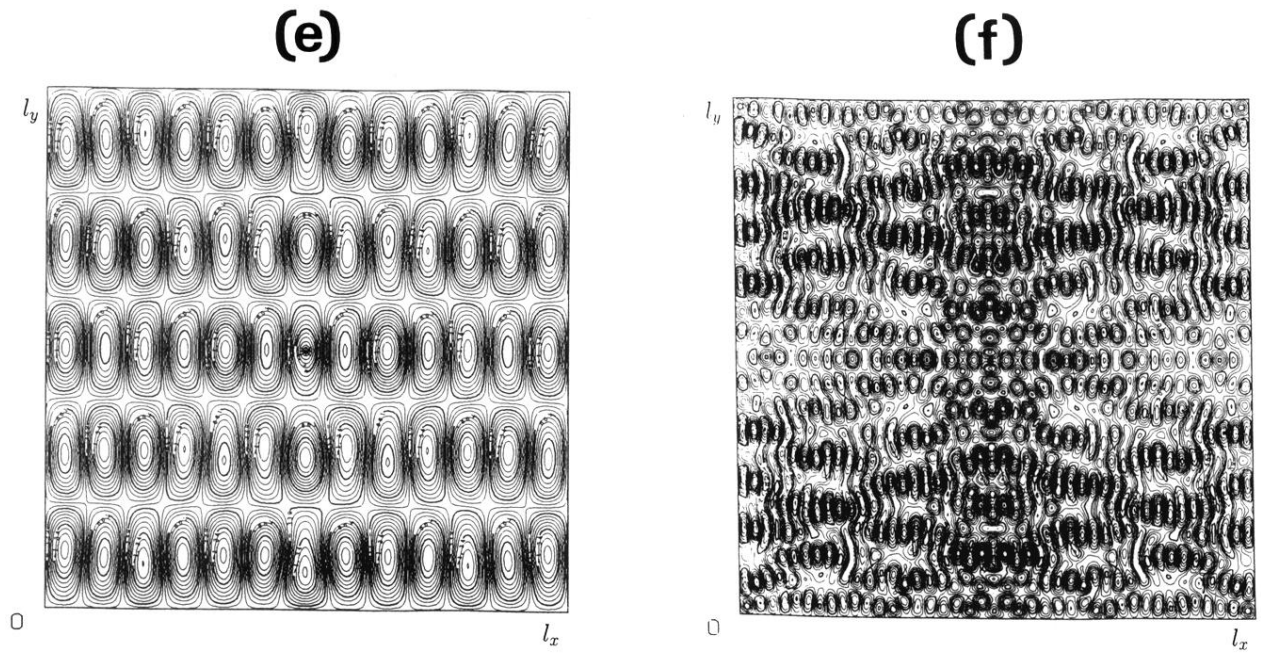

FIG. 3. (*Continued*).